JOURNAL OF CATALYSIS 47, 1–10 (1977)

Catalysis of Carbon Monoxide and Carbon Dioxide Methanation by $CeAl_2$, $CeCo_2$, $CeNi_2$, Co, and Ni[1]

C. A. LUENGO, A. L. CABRERA, H. B. MACKAY, AND M. B. MAPLE

Institute for Pure and Applied Physical Sciences, University of California, San Diego, La Jolla, California 92093

Received January 30, 1976; revised December 17, 1976

The catalytic activity of the three isostructural compounds $CeAl_2$, $CeCo_2$, and $CeNi_2$ and of pure Co and pure Ni for the methanation of carbon monoxide and carbon dioxide was measured with a microcatalytic technique between 100 and 800°C. The $CeCo_2$ and $CeNi_2$ compounds decomposed during exposure to reaction conditions—$CeCo_2$ into a mixture of CeO_2 and free Co, and $CeNi_2$ into a mixture of CeO_2 and free Ni. In their decomposed states, $CeCo_2$ and $CeNi_2$ had activities for methanation which are comparable to those of pure Co and pure Ni, and they were generally more selective than pure Ni and pure Co towards the formation of hydrocarbons of molecular weight exceeding that of methane. Although the $CeAl_2$ catalyst exhibited only moderate activity for methanation in comparison to the other catalysts which were investigated, it was the most stable with respect to sintering—diminution of its activity by sintering effects was observed only above 700°C. Arrhenius type plots were generally found to be linear.

INTRODUCTION

A large class of intermetallic compounds with the formula AB_2 crystallize in the face-centered cubic $MgCu_2$ crystal structure (C15) (*1*). Since the number of possible combinations of A and B atoms is quite large, we sought to examine the catalytic activity of various AB_2 isostructural compounds for the hydrogenation of carbon monoxide and carbon dioxide into methane to determine which combinations of elements with the C15 structure constitute the most active catalysts. This paper reports our intial results for the C15 compounds $CeAl_2$, $CeCo_2$, and $CeNi_2$. We also report measurements of methanation activity on pure Co and pure Ni to provide familiar standards with which our results for C15 compounds can be compared.

[1] Research supported by the National Science Foundation under Grant No. NSF DMR74-03838.

EXPERIMENTAL DETAILS

The microcatalytic technique first described by Kokes *et al.* (*2*) was employed to measure the *relative* activities of the catalyst materials which were investigated. In this study, the microcatalytic technique was intended to serve as a purely qualitative method to rapidly compare the activities of different catalysts under the same experimental conditions. No effort was made to establish the reaction order or compare results to steady-state data; this precluded any *quantitative* interpretation of kinetic parameters (e.g., activation energy) derived from these results as shown, for example, by Bett and Hall (*3*).

In our apparatus (Fig. 1), a carrier gas was flowed over the sample, which was situated in a temperature controlled reactor, and then into a gas chromatograph vented to the atmosphere. The gas pressure

ISSN 0021-9517

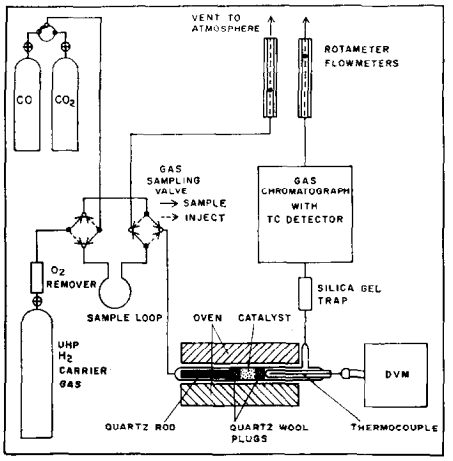

FIG. 1. Schematic diagram of the gas chromatograph–microcatalytic reactor system.

in the reactor was equal to 1.2 atm for the carrier gas flow rates normally used. A pulse of the reactant gas mixture of known volume (0.5 scc) was injected into the carrier gas before it entered the reactor by means of a Hewlett-Packard gas sampling valve. The reactor consisted of a 6 mm o.d. × 4 mm i.d. × 30 cm long quartz tube in a 10 in. tube furnace, the temperature of which could be regulated to within ±1°C of a preset value. The powdered sample was held in the reactor tube with quartz wool plugs. A thermocouple enclosed in a thin-walled 3 mm o.d. quartz tube was inserted in one side of the reactor tube, making direct contact with the sample to monitor its temperature. The products of the reacted pulse were then resolved by the gas chromatograph, a Hewlett-Packard 5700A with a thermal conductivity detector heated to 150°C and a 10 ft 0.25 in. diam column of Porapak Q, temperature programmed between −40 and +150°C. The chromatograph peak of water tailed so badly that the water had to be removed with a silica gel trap which was located between the reactor exhaust and the gas chromatograph.

In initial experiments, helium was used as the carrier gas, and the injected pulse consisted of a mixture of H_2 and CO, or H_2 and CO_2. This procedure proved unsatisfactory since the pulses were at first completely chemisorbed until the surface of the sample was saturated, and even when products were obtained the carbon balance was history dependent. When H_2 was used as the carrier gas at a flow rate of 50 scc/min (as measured by a rotameter) and pulses of pure CO or CO_2 were injected, the carbon balance was good and conversions were reproducible. Therefore, this latter technique was adopted for all the measurements reported here. The gases used in this work had the following purities: H_2, 99.999%; CO, 99.3%; CO_2, 99.995%. The 0.5 scc volume of the CO or CO_2 pulse was small enough to allow thorough mixing with the H_2 carrier for complete conversion of the reactants to CH_4 whenever the catalyst activity was sufficiently high. Despite the strong exothermic nature of these methanation reactions, no more than a 2°C increase in catalyst temperature was observed. Without a catalyst in the reactor, no product CH_4 was detected when CO or CO_2 was injected into the H_2 carrier stream for reactor temperatures up to 800°C.

Samples of $CeAl_2$, $CeCo_2$, and $CeNi_2$ were prepared by arc melting in high purity argon. The resulting ingots, which weighed about 5 g, were crushed and passed through a 400 mesh sieve. This yielded a powder with a maximum particle diameter of 38 μm. The powders were X-rayed and found to have the characteristic C15 crystal structure with lattice parameters in good agreement with values previously reported in the literature (see Table 1). The compounds were prepared from starting materials of 99.9% pure Ce and 99.999% pure Al, Co, and Ni. The Ni sample was prepared by reducing 99.999% pure NiO powder in the reactor tube with a stream of H_2 (500 scc/min) for 16 hr at 450°C. The resulting material was then powdered and sieved through 400 mesh. The Co sample was made from 99.999% pure Co sponge which was reduced in H_2 and powdered in the

TABLE 1

Catalyst	Before exposure to reaction						After exposure to reaction					
	Crystal structure	Lattice parameter (Å)	N_2 BET area (m^2/g)	Ar BET area (m^2/g)	H_2 area (m^2/g)	CO area (m^2/g)	Crystal structure	Lattice parameter (Å)	N_2 BET area (m^2/g)	Ar BET area (m^2/g)	H_2 area (m^2/g)	CO area (m^2/g)
$CeAl_2$	C15	8.060	0.50	—	—	—	Same	Same	0.32	—	—	0.25
$CeCo_2$[a]	C15	7.160	0.12	0.08	—	0.012	Unstable	—	0.35	0.37	—	0.23
$CeNi_2$	C15	7.208	0.42	—	—	0.04	Unstable	—	3.12	—	—	1.05
Ni	fcc	3.528	0.71	0.28	0.27	—[b]	Same	Same	0.66	—	0.26	—[b]
Co	hcp	1.623	0.32	0.44	0.18	—[b]	Same	Same	0.27	0.36	0.23	—

[a] This specimen was sieved to particle diameters between 38 and 63 μm.

[b] No values are given here because the H_2 areas for Co and Ni were used to derive the effective areas per CO molecule as explained in the text.

same manner as the Ni sample. The pretreatment of all the samples involved initially cleaning the sample surface *in situ* by reduction in the hydrogen carrier gas at a temperature higher than that required for total conversion of CO or CO_2 to methane by the particular sample. In the case of $CeNi_2$ and $CeCo_2$ which decomposed, as discussed below, CO_2 pulses were injected over the samples until reproducible methanation results were obtained. Otherwise there were no significant temperature hysteresis effects in the data for any of the samples. This was not surprising since between consecutive CO or CO_2 pulses the sample remained for 30 min at high temperature in the stream of highly purified H_2 carrier gas. This was done to avoid the accumulation of contaminants on the catalyst surface which could be introduced with each pulse due to the relatively lower purity of CO or CO_2. Any build-up of carbon due to carbon forming reactions is also precluded by this continuous hydrogenation procedure.

The BET method (*4*) was employed to measure surface areas using N_2 and Ar, and a volumetric adsorptometer based on the design of Benson and Garten (*5*). Sensitivity was improved by using a Baratron capacitance manometer to measure the pressure, permitting reproducible determination of areas as low as 0.1 m^2 to within 20%.

Active areas were also measured for each catalyst, using a temperature programmed desorption technique (*6*). The measurements were performed *in situ* in the gas chromatograph–microcatalytic reactor system. A two position gas sampling valve was connected to the tubular reactor which, in one position, connected the reactor directly to the gas chromatograph, and, in the other position, isolated the reactor so that the catalyst could be subjected to a constant pressure of the H_2 or CO adsorbate gases. The Ni and Co samples were cleaned in a stream of flowing hydrogen in the same manner employed in their pretreatment prior to measuring their catalytic activity, whereas the C15 compounds were cleaned in a stream of flowing helium in order to avoid the formation of hydrides. After cleaning, the samples were exposed to the H_2 or CO adsorbate gases at room temperature and at pressures between 1 and 2 atm for at least 0.5 hr. Next, the reactor was connected to the gas chromatograph so that the UHP carrier gas could sweep any physisorbed gases from the surface of the sample. Finally, the temperature was programmed to increase linearly with time at a rate of 50°C/min to drive the residual chemisorbed gas off the catalysts and into the carrier stream. The volume of gas desorbed was measured with the thermal conductivity detector of the gas chromatograph with the column removed. The carrier gases were argon for the hydrogen desorption measurements and helium for the carbon monoxide desorption measurements. The

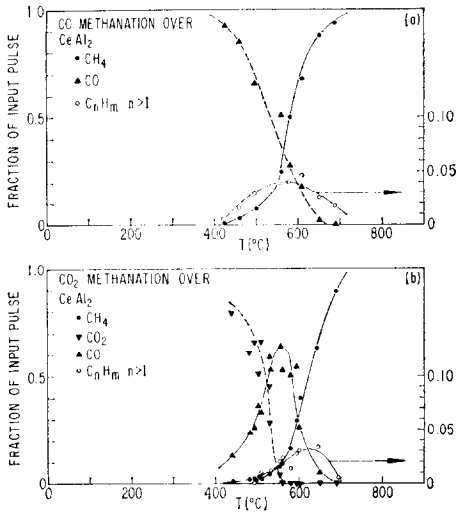

FIG. 2. Plots of fraction of input pulse vs temperature for (a) carbon monoxide and (b) carbon dioxide methanation over $CeAl_2$. Sample weight: 1.3 g.

H_2 and CO purities were the same as stated above. The helium and argon purities were 99.999 and 99.998%, respectively.

Both H_2 and CO desorption measurements were made for pure Co and pure Ni; whereas only CO desorption measurements were made for the C15 compounds since they readily *absorbed* hydrogen. The specific areas for the various catalysts are tabulated in Table 1.

RESULTS AND DISCUSSION

The CO and CO_2 methanation reactions,

$$CO + 3H_2 \rightleftharpoons CH_4 + H_2O, \qquad (1)$$

and

$$CO_2 + 4H_2 \rightleftharpoons CH_4 + 2H_2O, \qquad (2)$$

were studied over powders of $CeAl_2$, $CeCo_2$, and $CeNi_2$. Ni and Co powders were also measured under the same experimental conditions to provide standards for comparison.

Plots of product gas (expressed as "fraction of input pulse") vs temperature for reaction products and reactants are shown in Figs. 2–6 for the materials investigated. The "fraction of input pulse" is defined as the moles of molecule produced per mole of CO or CO_2 introduced as calculated from the ratio of the STP volume of the resolved product eluted from the gas chromatograph and the STP volume of the injected CO or CO_2 pulse.

Shown in Fig. 2a are the data for the methanation of CO over the $CeAl_2$ catalyst. Between about 400 and 700°C, one or more light hydrocarbons (C_nH_m, $n > 1$) are produced with a yield which reaches a maximum fractional conversion of 0.04 at the temperature where CH_4 conversion is about 50%. Of the three minor peaks due to the higher hydrocarbons which appeared in the chromatograms, we were able to identify two; one with C_2 hydrocarbons and another with C_3 hydrocarbons. Presented in Fig. 2b are the results for the methanation of CO_2 over $CeAl_2$. In addition to CH_4, CO and one or more light hydrocarbons are produced. The CO yield reaches a maximum fractional conversion of 0.65 and the light hydrocarbon yield exhibits a maximum of 0.03. The CO is probably produced by the water–gas shift reaction:

$$CO_2 + H_2 \rightleftharpoons CO + H_2O. \qquad (3)$$

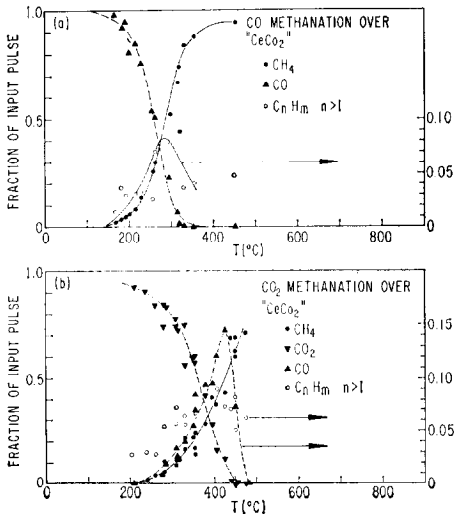

FIG. 3. Plots of fraction of input pulse vs temperature for (a) carbon monoxide and (b) carbon dioxide methanation over "$CeCo_2$" (the quotation marks denote compounds that decomposed during exposure to reaction conditions). Sample weight: 0.82 g.

The curves of Fig. 2b suggest that the temperature of the reactor must be high enough for appreciable CO_2 conversion to CO by means of the above reaction before there is a significant CH_4 yield. Consequently, the methane conversion and peak in light hydrocarbon yield occur at higher temperatures than for CO methanation.

The yields of methane in the fraction of input pulse vs temperature plots for CO methanation (Fig. 2a) and CO_2 methanation (Fig. 2b) over $CeAl_2$ in the range ~600–700°C appear to exceed somewhat their equilibrium values (*7*, *8*) for their respective stochiometric hydrogen–carbon oxide ratios of 3:1 and 4:1. This may easily occur in the microcatalytic reactor for two reasons. First, an absence of steady-state conditions in the microcatalytic reactor results in relative reactant concentrations which vary with time and position in the catalyst bed and the H_2 carrier constantly dilutes the carbon oxide pulse. Second, the catalyst is saturated with hydrogen before injection of each CO or CO_2 pulse into the hydrogen carrier stream. These conditions may lead to an average H_2–CO or H_2–CO_2 ratio that is greater than the respective stochiometric values of 3:1 and 4:1, which favors higher equilibrium methane yields.

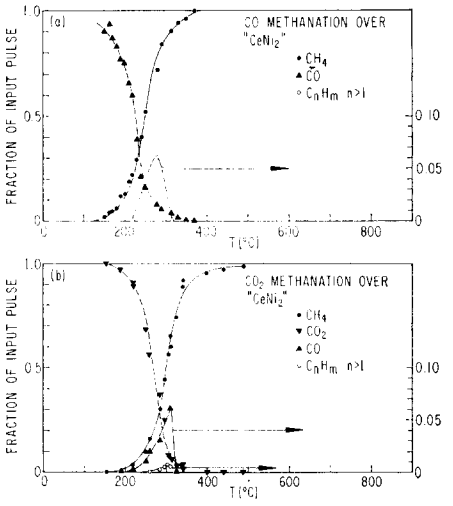

FIG. 4. Plots of fraction of input pulse vs temperature for (a) carbon monoxide and (b) carbon dioxide methanation over "$CeNi_2$" (the quotation marks denote compounds that composed during exposure to reaction conditions). Sample weight: 3.5 g.

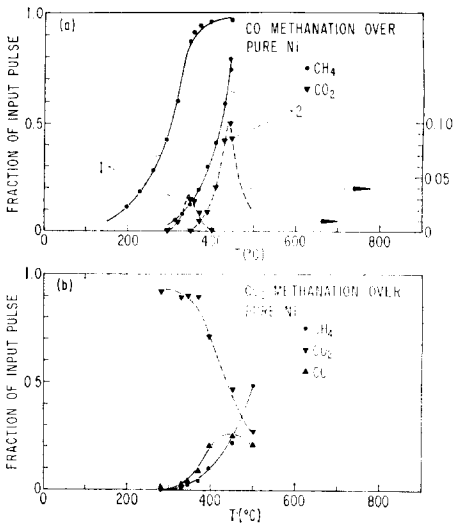

FIG. 5. Plots of fraction of input pulse vs temperature for (a) carbon monoxide and (b) carbon dioxide methanation over pure Ni. Sample weights: (1) 0.26 g, (2) 0.10 g.

The X-ray patterns for $CeAl_2$, after the powder was exposed to reaction conditions at temperatures up to 800°C, revealed that no significant crystallographic changes had occurred during the course of the studies. A small reduction in the BET area for $CeAl_2$ (Table 1) is attributed to an increase in particle size due to sintering. Some extra lines were present after exposure, indicating the formation of minor components consisting of cerium aluminum oxides.

In contrast, $CeNi_2$ and $CeCo_2$ decomposed during exposure to reaction conditions—$CeNi_2$ into CeO_2 and Ni, and $CeCo_2$ into CeO_2, α-Co (hexagonal), and β-Co (fcc)—as revealed by X-ray patterns taken after completion of the experiments. A partially oxidized $CeCo_2$ sample also contained CeH_2, a possible intermediate in the process of decomposition. We denote these two materials as "$CeCo_2$" and "$CeNi_2$" since their characteristics (crystal structure, surface area, etc.) changed during the methanation experiments.

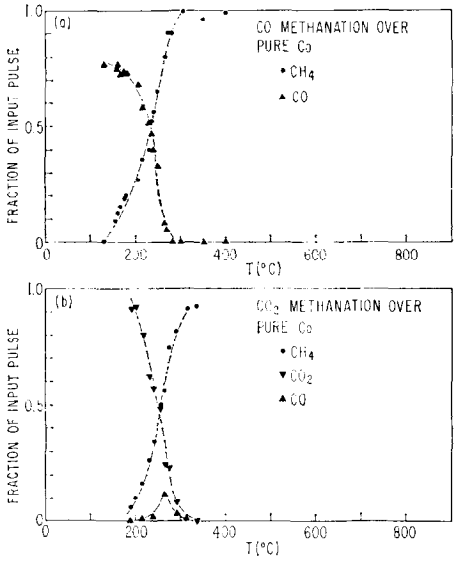

FIG. 6. Plots of fraction of input pulse vs temperature for (a) carbon monoxide and (b) carbon dioxide methanation over pure Co. Sample weight: 0.53 g.

The large increase in BET area (Table 1) for "$CeNi_2$" and "$CeCo_2$" as a result of decomposition was further investigated using a scanning electron microscope. The "$CeNi_2$" particles, whose surfaces before decomposition were smooth and rounded, appeared still intact but heavily incrusted with small, rough grains on top of a finely fissured, undulated surface, consistent with the eightfold increase in area. The "$CeCo_2$" particles which had smooth, flatly cleaved surfaces before decomposition, were also still intact but crisscrossed with deep crevices. Surface roughness was visible only under high magnification. Thus, the three- to fivefold area increase of "$CeCo_2$" is due primarily to the heavy cracking, probably caused by lattice expansion after hydrogen absorption and hydride formation by Ce, as found in the X-ray pattern and similar to the cracking observed in the pure rare earths (*9*).

The results for CO methanation over "$CeCo_2$" are given in Fig. 3a. As in the case of $CeAl_2$, a peak in the light hydrocarbon yield occurs near a methane concentration of 50%. However, complete methane conversion occurs at a temperature 300°C less than that for $CeAl_2$. The curves for CO_2 methanation over "$CeCo_2$" in Fig. 3b indicate a small, symmetric CO peak near 50% methane conversion with the yield falling to zero at the same temperature as the CO_2 concentration. Unless the light hydrocarbons produced are distributed with $n > 2$, the carbon balance appears to be particularly bad at the highest temperatures; possibly a result of carbon deposition.

The methanation curves for "$CeNi_2$," shown in Figs. 4a and b, are qualitatively similar to those of "$CeCo_2$" although conversions occur at slightly lower temperatures. However, the CO and light hydrocarbon yields for CO_2 methanation appear to be much reduced compared to CO_2 methanation over "$CeCo_2$."

In a separate experiment, the stability of CeO_2 at high temperature and in the H_2 reducing atmosphere was checked by keeping the sample under inert atmosphere until

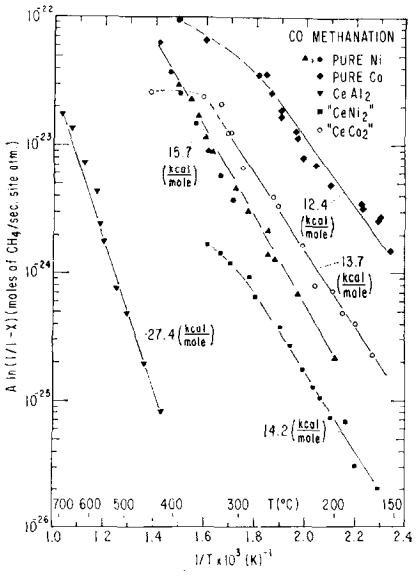

FIG. 7. Arrhenius-type plots for carbon monoxide methanation over Ni, Co, $CeAl_2$, "$CeNi_2$," and "$CeCo_2$" (the quotation marks denote compounds that decomposed during exposure to reaction conditions). The *apparent* activation energy for the linear region of each plot is indicated in the figure.

the X-ray pattern was obtained. The CeO_2 sample was also found to be inactive for CO methanation up to ~600°C.

Figures 5 and 6 present methanation data obtained using pure Ni and pure Co as catalysts under the same experimental conditions as for the C15 compounds. Compared to the compounds, the most obvious difference is the lack of light hydrocarbons in the reaction products. Of note are the results of CO methanation over Ni in Fig. 5a. Small peaks of CO_2 appear, again due to the water–gas shift reaction, which did not appear in the CO methanation products of any of the compounds, including the decomposed "$CeNi_2$" which contained free Ni. Figure 5a also demonstrates the effect of changing the sample size, with the smaller sample converting at higher temperature and thereby enhancing the water–gas shift yield of CO_2.

Small reductions in the BET areas for pure Ni and pure Co (Table 1) are attributed to an increase in grain size due to sintering. In Ni powders this is known to occur when the sample is exposed to temperatures greater than 400°C (*10*).

In an attempt to qualitatively compare the relative activities of the materials investigated, plots of $\ln [A \ln (1/1 - x)]$ vs $1/T$ for CO and CO_2 methanation were constructed and are shown in Figs. 7 and 8, respectively. In this formula x represents the fractional conversion of the CO or CO_2 input pulse to CH_4. The constant A is equal to F/RTN where F is the flow rate of the reactants, R is the gas constant per mole, and N is the total number of active sites of the sample. For a first order reaction, it has been shown that the quantity $A \ln (1/1 - x)$ is equal to the product kK, where k is the first order rate constant of the surface reaction and K is the adsorption equilibrium constant (*11*). However, since we do not know the orders of the methanation reactions over the catalysts we have investigated, we stress that the purpose of the plots shown in Figs. 7 and 8 is to compare the various catalysts with one another and to illustrate the striking features. The *apparent* activation energies given in Figs. 7 and 8 which have been derived from the Arrhenius-type plots should not be regarded as quantitative indices for the reactions unless further investigations should show that such an interpretation is justifiable from the standpoint of the reaction kinetics.

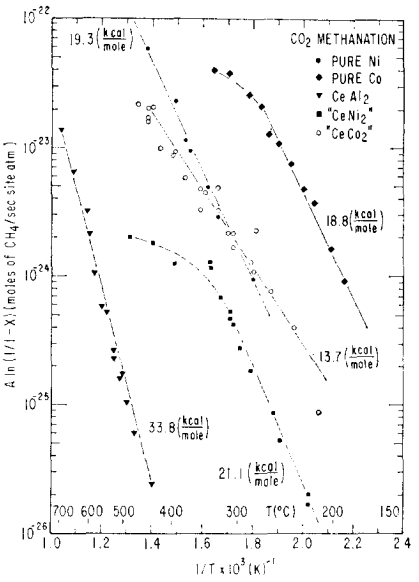

FIG. 8. Arrhenius-type plots for carbon dioxide methanation over Ni, Co, $CeAl_2$, "$CeNi_2$," and "$CeCo_2$" (the quotation marks denote compounds that decomposed during exposure to reaction conditions). The *apparent* activation energy for the linear region of each plot is indicated in the figure.

In order to express the reaction rate constant data shown in Figs. 7 and 8 in terms of "turnover numbers" (number of molecules reacting per active site and per unit time), the active areas of the catalysts were measured *in situ* in the gas chromatograph–microcatalytic reactor system as described in the section on experimental details. The active areas of pure Co and pure Ni were deduced from the volume of chemisorbed hydrogen v_{H_2} assuming that each hydrogen atom adsorbed to a single site and occupied an area of 6.2 Å^2. The active areas of $CeAl_2$, "$CeCo_2$," and "$CeNi_2$" were estimated

from the volume of chemisorbed carbon monoxide v_{CO}, since all of the compounds readily *absorbed* hydrogen. Because carbon monoxide often forms "bridged" as well as "linear" chemisorption bonds with the surface atoms of metals (*12*), the effective areas of a chemisorbed CO molecule were "calibrated" from the hydrogen active areas. The active area of "$CeCo_2$" was estimated from the CO on Co active area calibration, while the active areas of $CeAl_2$ and "$CeNi_2$" were derived from the CO on Ni active area calibration. The v_{CO}/v_{H_2} ratios were found to be equal to 1.61 for Co and 1.07 for Ni. This indicates that most of the CO molecules chemisorb to single sites on Co and to double sites on Ni. The active areas for the five catalysts are given in Table 1. It is interesting to note that the active area of "$CeNi_2$" increased by a factor of 26, whereas its BET area only increased by a factor of 7–8.

The data of Figs. 7 and 8 indicate the following general trends with respect to increasing activity (at the higher temperatures): (a) $CeAl_2$ < "$CeNi_2$" < Ni < "$CeCo_2$" < Co for CO methanation; (b) $CeAl_2$ < "$CeNi_2$" < "$CeCo_2$" $\lesssim$ Ni < Co for CO_2 methanation; (c) CO_2 methanation activities are smaller than CO methanation activities for all of the catalysts. The last feature (c) may be attributable to the weaker chemisorption on metals of CO_2 with respect to CO (*12*).

Each Arrhenius plot was made from data that ranged from close to zero conversion to nearly complete conversion. In some cases (e.g., Ni), the Arrhenius plots spanned as much as three orders of magnitude in rate constant. Since it is unlikely that the reaction rates are diffusion limited at close to zero conversion, the linearity of all but two of the Arrhenius plots from low to high conversion suggests that the rates are not limited by diffusion. However, there is some evidence for diffusion limiting at high temperatures in two of the Arrhenius-type plots. For CO methanation over "$CeCo_2$," there is an abrupt saturation of the rate constant above ~350°C, while for CO_2 methanation over "$CeNi_2$," there is a more gradual saturation of the rate constant above ~300°C. These examples reveal the temperature regime in which diffusion limiting would be *expected* to occur and support the assumption that the reaction rates for low conversion are *not* diffusion limited.

Additional evidence for the lack of diffusion limiting results from our studies of CO methanation over Ni. In this case, two Ni samples of different weights were measured, and, as expected, the smaller sample yielded methane at correspondingly higher temperatures than the larger sample. The resultant CO methanation Arrhenius-type plot for the larger sample was coincident with that of the smaller sample in the temperature range where the data overlapped so that the *same* specific rate constant characterized both the high conversion data for the larger sample and the low conversion data for the smaller sample. This indicates that the rate for CO methanation is directly proportional to the *weight* of the catalyst, a feature of reactions for which the rate is governed by actual reaction mechanisms rather than by diffusion (*13*).

It should be noted that the quantity $A \ln (1/1 - x)$ has only been shown to be equal to the product kK when the reaction is first order, although, even if the quantity $A \ln (1/1 - x)$ could be identified with the product kK, the values of E_{app} determined here could not be related *quantitatively* to steady-state data which yield the surface reaction rate constant k since the relevant adsorption equilibrium constants K for mixtures of CO or CO_2 and H_2 are not known. For cases where the adsorption is sufficiently small, K is proportional to $\exp(-\Delta H_a/RT)$ where ΔH_a, the enthalpy of adsorption, is negative, and the true activation energy E is therefore always *larger* than the apparent activation energy E_{app}; i.e., $E = E_{app} - \Delta H_a$ (*13*). This may account for the fact that the apparent ac-

tivation energy for CO methanation over Ni (15.7 kcal/mole) from this work is considerably lower than the values previously reported in the literature [28 kcal/mole (*14*) and 28–31 kcal/mole (*15*)] from initial rate measurements made in a differential reactor, assuming that the kinetics of the reaction warrant such a quantitative interpretation of the apparent activation energies derived from the microcatalytic technique we have employed. It should be noted, however, that the literature values refer to measurements made on "supported" Ni catalysts, and it is often found that "inert" supports are not completely inert (*12*). Nevertheless, the apparent activation energy for CO methanation over Ni determined here is definitely smaller than the steady-state value, which is qualitatively consistent with expectations when adsorption of reactants onto the surface is taken into account.

SUMMARY

We have measured the relative catalytic activities of the three isostructural cubic Laves phase (C15) compounds $CeAl_2$, $CeCo_2$, and $CeNi_2$ and of pure Co and pure Ni for the methanation of carbon monoxide and carbon dioxide by means of the microcatalytic technique between 100 and 800°C.

The $CeCo_2$ and $CeNi_2$ compounds were found to decompose during exposure to reaction conditions—$CeCo_2$ into a mixture of CeO_2 and free Co, and $CeNi_2$ into a mixture of CeO_2 and free Ni. In their decomposed states, $CeCo_2$ and $CeNi_2$ had activities for methanation which are comparable to those of pure Co and pure Ni, and they were generally more selective than pure Ni and pure Co towards the formation of hydrocarbons of molecular weight exceeding that of methane.

The $CeAl_2$ compound, which did *not* decompose under reaction conditions, exhibited only moderate activity for methanation in comparison to the other catalysts which were investigated (including Co and Ni). However, it was the most stable with respect to sintering—diminution of its activity by sintering effects was observed only above 700°C.

The relative activities of the various catalysts were determined by converting the relative concentration vs temperature plots into Arrhenius-type plots in the manner described above. The primary purpose of constructing the Arrhenius-type plots was to compare *qualitatively* the activities of the $CeAl_2$, "$CeCo_2$," and "$CeNi_2$" catalysts with one another and with the pure Co and pure Ni reference catalysts.

Some of the more interesting results to emerge from this investigation center on the properties of the compound $CeAl_2$. This catalyst has been found to be moderately active for CO and CO_2 methanation and to be resistant to decomposition and sintering under reaction conditions up to ~700°C. The catalytic activity and stability of $CeAl_2$ suggest that it might therefore be fruitful to study dialuminides of other rare earth elements, and possibly even actinide elements (e.g., $ThAl_2$ and UAl_2) as potential methanation catalysts.

On the other hand, the fact that the $CeCo_2$ and $CeNi_2$ compounds decompose under reaction conditions into CeO_2 and free Co or Ni does not imbue these catalysts with any important properties which make them superior to pure Co or Ni for the methanation of carbon oxides, with the possible exception of their tendency in their decomposed states to be somewhat more selective than Co and Ni for the production of hydrocarbons with molecular weights exceeding that of methane. It seems quite likely that most or even all of the other existing Laves phase compounds of the formula $RE(TM)_2$ where TM denotes a transition metal element also decompose under reaction conditions and that they, too, will not constitute attractive catalysts for the methanation of the oxides of carbon.

REFERENCES

1. Pearson, W. B., "Handbook of Lattice Spacings and Structures of Metals and Alloys," Vol. 2. Pergamon Press, 1967.
2. Kokes, R. J., Tobin H., Jr., and Emmett, P. H., *J. Amer. Chem. Soc.* **77**, 5860 (1955).
3. Bett, J. A. S., and Hall, W. K., *J. Catal.* **10**, 105 (1968).
4. Brunauer, S., Emmett, P. H., and Teller, E., *J. Amer. Chem. Soc.* **60**, 309 (1938).
5. Benson, J. E., and Garten, R. L., *J. Catal.* **20**, 416 (1970).
6. Cvetanovic, R. J., and Amenomiya, Y., *in* "Advances in Catalysis" (D. D. Eley, H. Pines, and P. B. Weisz, Eds.), Vol. 17, p. 103. Academic Press, New York, 1967.
7. Greyson, M., Demeter, J. J., Schlesinger, M. D., Johnson, G. E., Jonakin, J., and Myers, J. W., "Synthesis of Methane," reprinted from Bureau of Mines Report of Investigations 5137, July, 1955.
8. Lunde, P. J., and Kester, F. L., *J. Catal.* **30**, 423 (1973).
9. Mulford, R. N. R., and Holley, C. E., Jr., *J. Phys. Chem.* **59**, 1222 (1955).
10. Carter, J. L., Cusumano, J. A., and Sinfelt, J. H., *J. Phys. Chem.* **70**, 2257 (1966).
11. Bassett, D. W., and Habgood, H. W., *J. Phys. Chem.* **64**, 769 (1960).
12. Bond, G. C., "Catalysis by Metals." Academic Press, London, 1962.
13. Bond, G. C., "Heterogeneous Catalysis: Principles and Applications," Clarendon Press, Oxford, 1974.
14. Dalla Betta, R. A., Piken, A. G., and Shelef, M., *J. Catal.* **35**, 54 (1974).
15. Dalla Betta, R. A., Piken, A. G., and Shelef, M., *J. Catal.* **40**, 173 (1975).